Research Article

Structural and Electrical Studies on ZnO-Based Thin Films by Laser Irradiation

Shanyue Zhao,[1] Yinqun Hua,[1,2] Ruifang Chen,[2] Jian Zhang,[1] and Ping Ji[1]

[1]*School of Material and Science Engineering, Jiangsu University, Zhenjiang 212013, China*
[2]*School of Mechanics Engineering, Jiangsu University, Zhenjiang 212013, China*

Correspondence should be addressed to Yinqun Hua; huayq@ujs.edu.cn and Ruifang Chen; crf0504@aliyun.com

The effects of laser irradiation on the structural and electrical properties of ZnO-based thin films were investigated. The XRD pattern shows that the thin films were highly textured along the *c*-axis and perpendicular to the surface of the substrate. Raman spectra reveal that Bi_2O_3 segregates mainly at ZnO-ZnO grain boundaries. After laser irradiation processing, the grain size of the film was reduced significantly, and the intrinsic atomic defects of grain boundaries and Bi element segregated at the grain boundary were interacted frequently and formed the composite defects of acceptor state. The nonlinear coefficient increased to 24.31 and the breakdown voltage reduced to 5.34 V.

1. Introduction

ZnO varistors exhibit high nonlinear coefficient, low leakage current, and high surge absorbing ability. They have been extensively applied on high-voltage protection of electrical equipment since the 1970s, such as inhibiting lightning over-voltage of electrical power system [1–5]. However, modern-day electronic components, mainly based on silicon, are more susceptible not only to electrical overvoltage transients, but also to damage by electromagnetic pulses or electromagnetic interference (EMI) noise that is now strictly regulated by law throughout the world [6, 7]. Therefore, the industry has high demands for low-voltage varistors. For a low-voltage varistor, it is required to be of few microns in thickness to reduce nonlinear voltage. ZnO films with good quality were grown through different methods, such as hydrothermal method [8], sol-gel technique [9], electron-beam evaporation [10], pulse laser deposition [11], and magnetron sputtering [12]. Among all, magnetrons puttering shows several advantages such as good adhesion between film and substrate, low substrate temperature, scalability to large areas, great thickness uniformity with a deposition rate range, and high film density [12–15].

Recently, laser irradiation technique has been used on thin films as an efficient method to improve the crystalline quality and increase the electron donors [16–19]. Laser irradiation has several advantages, including fast crystallization at room temperature, possibility of local crystallization, crystallization of thin films on low melting point substrates, and increasing charge carriers through a photoconductivity effect. Tsay and Wang [18] performed ZnO thin films on glass by sol-gel and used KrF excimer laser for annealing. They reported that the crystallinity levels and average crystallite size of thin films with excimer laser irradiation were greater than those of thermally annealed thin films. Tsang et al. [19] fabricated transparent conducting AZO thin films using KrF excimer laser irradiation. They reported that the electrical and optical characteristics of AZO thin films irradiated by excimer laser improved significantly.

To the best of our knowledge, no report on ZnO-based thin film varistors with laser irradiation for low-voltage application exists. In our previous work [20], we studied the effect of laser shock on electrical property of ZnO varistor ceramics. In the present work, ZnO-based thin films of high quality were prepared by RF magnetron sputtering technique on Si (111) substrates. After examinations, the films were subsequently treated by laser irradiation. The paper has studied the structural and electrical properties of the ZnO-based thin film varistors for low-voltage application.
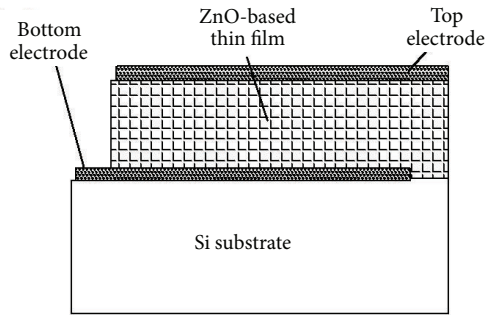
FIGURE 1: The structure of the ZnO-based thin film varistors.

2. Experiment

ZnO-based thin films were deposited on Si (111) substrates by RF magnetron sputtering technique and followed by annealing at 700°C for 4 h in the air. The target, ZnO-based ceramic with 60 mm in diameter and 5 mm in thickness, was formed by dry pressing and subsequently sintered in the air. The raw materials of the target were mixed powders and the matching composition was 96.5 mol% ZnO + 2 mol% Bi_2O_3 + 1.5 mol% (MnO_2, Co_2O_3, Cr_2O_3, and Sb_2O_3). It is the optimized composition investigated by the authors in our previous works. Si (111) which was used as the substrate for ZnO thin films deposition were cleaned in an ultrasonic bath with ethanol for 15 min than dried for use. The substrates were sprayed gold in the metal-spraying equipment for 5 min, to prepare a layer of bottom electrode on the Si substrate. Using the sky-0826138 RF magnetron sputtering instrument, the background vacuum degree of the chamber was less than 1 $\times 10^{-4}$ Pa. The sputtering pressure was 3.0 Pa, and the Argon flow was 30 sccm. The sputtering time was 60 min, and the sputtering power was 150 W. The substrate temperature was 300°C. The film thickness was controlled within 2 microns. After the laser irradiation processing, the laser irradiation area was covered with gold to prepare the top electrode. Figure 1 shows the structure of the ZnO-based thin film varistors.

The 0.2 mm aluminum foil adhered to the film surface as the absorption layer. The homemade liquids were coated on the aluminum foil surface as the constraint layer. The thickness was 0.5 mm. The laser irradiation parameters are as followings: light spot diameter of 6 mm, wavelength of 1064 nm, pulse width of 5 ns, pulse energy of 0.8 J. Finally, the samples were set in the mold to conduct the laser irradiation experiment. After the laser irradiation processing, the films' surfaces were fine, which showed that as long as the parameters of laser irradiation were appropriate, laser irradiation could be applied on the films completely.

The structural properties were characterized by X-ray diffractometer (XRD) with CuKα radiation. The surface morphology and root mean square (RMS) roughness level of the films were examined by tapping atomic force microscope (AFM). Plane-view micrographs of ZnO-based thin films were taken with a field-emission scanning electron microscope (FE-SEM). Raman spectra were excited with the 532 nm line of a laser at an incident power of 10 mW and obtained in the range 0–3000 cm^{-1}. The J-V curves are measured by transistor characteristic meter. The breakdown voltage $U_{1\,mA}$ (V) and leakage current J_L (μA/mm^2) are measured by piezoresistor general measuring instrument.

3. Results and Discussions

The X-ray diffraction patterns of the ZnO-based thin films before and after irradiation are shown in Figure 2. Only the (002) peaks are observed in the XRD patterns, which shows that the films are highly textured along the c-axis and perpendicular to the surface of the substrate. This diffraction peak is indexed to those of hexagonal wurtzite zinc oxide and no diffraction peaks of any other phases or impurities are detected [8, 9, 11]. After irradiation, the intensity of (002) ZnO peak increases and there is a shift to larger angles. This trend with the shift of 2θ in XRD patterns suggests that the Bi^{3+} ions occupied the Zn^{2+} substitutional sites [15, 21]. This result also shows that laser irradiation can facilitate the substitution of Bi^{3+} ions to Zn^{2+} ions [18].

Figure 3 shows the AFM morphologies for the films, which illustrate the surface morphology of the thin films. (a) is the sample before irradiation and (b) is the sample after irradiation. After laser irradiation, the film surface morphology changes significantly. Corresponding to the above two samples, the RMS surface roughnesses are 31.4 and 2.8 nm. The film treated by laser irradiation has a relative smooth and dense surface morphology. At the initial state, the laser shock wave passes through the rigid aluminum foil adhering to the film surface and reaches the bottom of the aluminum foil. For the impedance mismatch of the aluminum foil and the film, strong contact pressure appears between the contact point of the aluminum foil and the film. The sharp protrusions are compressed at the strong contact pressure and this is characterized by the great reduction of surface roughness. Figure 4 shows the morphology and particle sizes of prepared film by SEM. The histograms reveal the distribution of average grain size, which are reasonably described by the Gaussian function, showing tight size distribution with average sizes of approximately 191 and 139 nm in diameter, respectively.

Figure 5 shows the Raman spectrum of ZnO-based thin film. A larger peak shift at 437 cm^{-1} is observed, which is almost the same position as the standard ZnO. It indicates that the thin film is almost free of stress. Theoretically, it is difficult to substitute Zn^{2+} by Bi^{3+} in ZnO crystal, for the radius of Bi^{3+} is much larger than Zn^{2+}. The former results indicate that Bi_2O_3 segregates mainly at ZnO-ZnO grain boundaries as Bi-rich phases during sintering in the ZnO-Bi_2O_3 system. The Bi elements distribute evenly throughout the thin film, and the distribution of Bi appears in certain regularity, which are almost distributed at the grain boundaries. After laser irradiation processing, grain boundaries increase with the grain refinement. In this condition, the intrinsic atomic defects of grain boundaries and Bi element segregated at the grain boundary interact frequently, forming the composite defects of acceptor state [22, 23]. So the interface state density
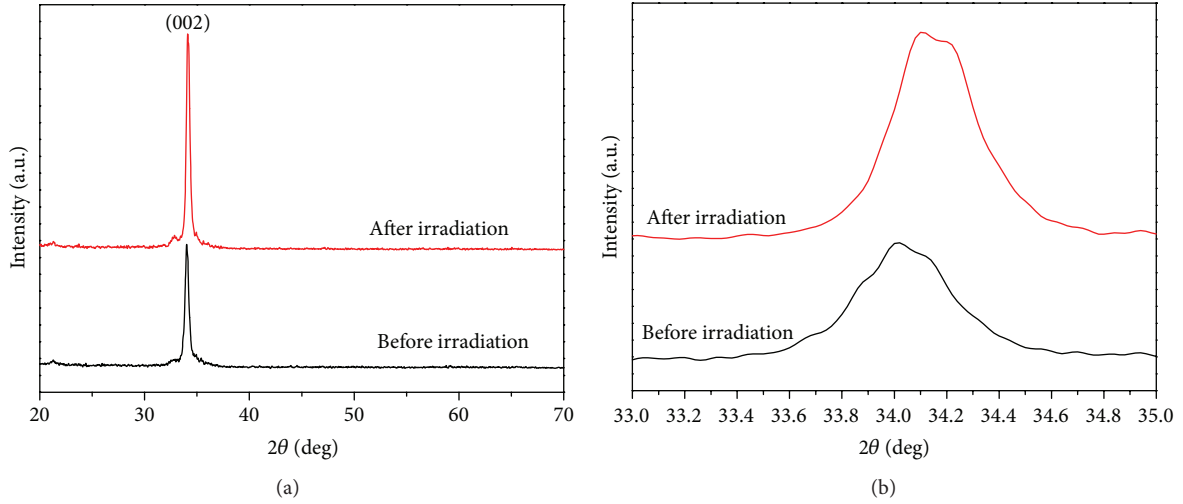
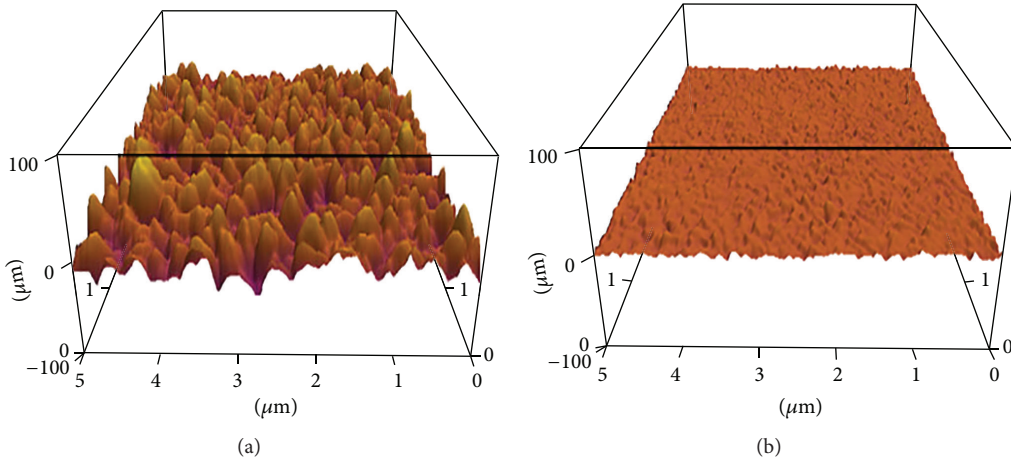Figure 2: XRD patterns of ZnO-based thin films.

Figure 3: AFM micrographs of the ZnO-based thin films.

N_S of grain boundaries increase greatly, which promotes the increasing of barrier height Φ_B and the nonlinear coefficient. Therefore, the pressure-sensitive electrical properties of ZnO-based ceramic film of laser irradiation state are excellent.

Table 1 is the result of electrical properties. The nonlinear coefficient is α, breakdown voltage is $U_{1\,mA}$ (V), and leakage current is J_L (μA/mm^2). After laser irradiation processing, the nonlinear coefficient is 24.31, which increases by 40.8%, and breakdown voltage is 5.34 V, which decreases by 20.7%. Leakage current density is as low as 2.03 μA/mm^2, which decreases by 12.1%. Similar investigations have been done by other researchers. Horio et al. [13] prepared the ZnO/Pr$_6$O$_{11}$ films on the glass substrates by the RF magnetron sputtering technique, and the film thickness was 600 nm/400 nm. The breakdown voltage was 20 V, and the nonlinear coefficient was 10. Miśta et al. [14] prepared the Bi-doped films on the ITO/Glass using Zn-Bi target by the RF magnetron sputtering technique. The results displayed that the breakdown voltage was from a few volts to dozens of volts, and the nonlinear

Table 1: Electrical properties of films before and after laser-irradiation processing.

Parameters	Before irradiation (I)	After irradiation (II)	Rate (%)
α	17.26	24.31	40.8
$U_{1\,mA}$ (V)	6.73	5.34	−20.7
J_L (μA/mm^2)	2.31	2.03	−12.1

coefficient was 15. Jeong [24] prepared low-voltage ZnO varistors and investigated the field failure; after polishing, the breakdown voltage was 9.71 V, and the nonlinear coefficient was 20.35. Therefore, the electrical properties improve significantly by the laser irradiation processing.

The grain boundary of ZnO-based ceramic film is a thin disorder area, where a large number of interface states and electron traps exist. They are able to capture the free electrons in the ZnO grains. The electrons of grain boundaries are
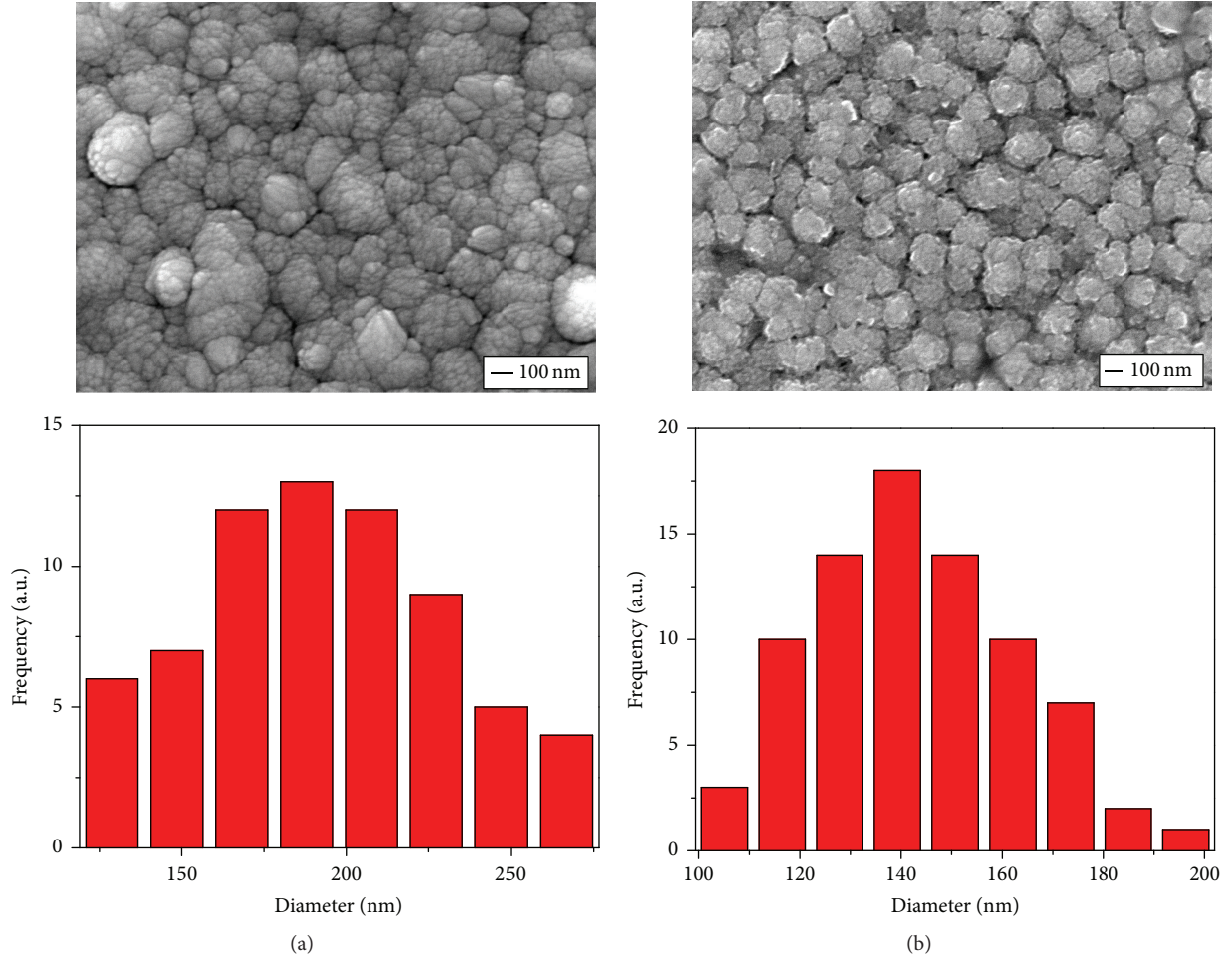
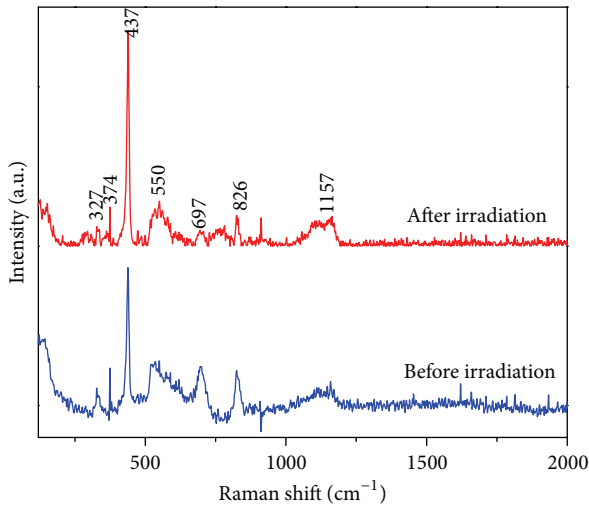FIGURE 4: SEM micrographs of the ZnO-based thin films.

FIGURE 5: Raman spectroscopy of ZnO-based thin films.

depleted, and depletion layers are formed. Consequently, electronic barriers with certain depth have been formed from grain surfaces into body. The barrier height is Φ_B, which is

called Double Schottky barrier [25]. It is the source of voltage-sensitive electrical property.

Nonlinear characteristics of ZnO-based film originate from the grain boundary barrier. To study the impact of laser irradiation processing on the electric properties of ZnO-based ceramic film, we adopted the double Schottky barrier model proposed by Gupta and Carlson [26] to explain the change of electrical property. At preswitch region, there is a relationship between the current density and the extra electric field obtained from the model, which is shown in [27]

$$J = AT^2 \exp\left[\frac{\left(\beta E^{0.5} - \Phi_B \right)}{(kT)} \right]. \tag{1}$$

J is current density, A is Richardson constant, T is absolute temperature, E is electric field intensity, Φ_B is barrier height, and K is Boltzmann constant. $\beta = \{1/(\gamma\omega)[2e^3/(4\pi\varepsilon_0\varepsilon_r)]\}^{1/2}$ [17], γ is grain number of unit length, ω is Barrier width, e is electron charge (1.602×10^{-19} C), ε_0 is vacuum dielectric constant (8.85×10^{-14} F/cm), and ε_r is relative dielectric constant (8.5). Setting T as 25°C, $\ln J$-$E^{0.5}$ fitting diagram of film and film of laser irradiation state are shown in Figure 5. The boundary characteristic

TABLE 2: The characteristic parameters of grain-boundary of ZnO-based ceramic films before and after laser-irradiation processing.

State	Barrier height Φ_B (eV)	Barrier width ω (Å)	Donor concentration N_D (10^{22} cm^{-3})	Density of interface states N_S (10^{14} cm^{-2})
Before irradiation (I)	1.86	1.13	13.5	15.3
After irradiation (II)	2.41	0.31	227	71.6
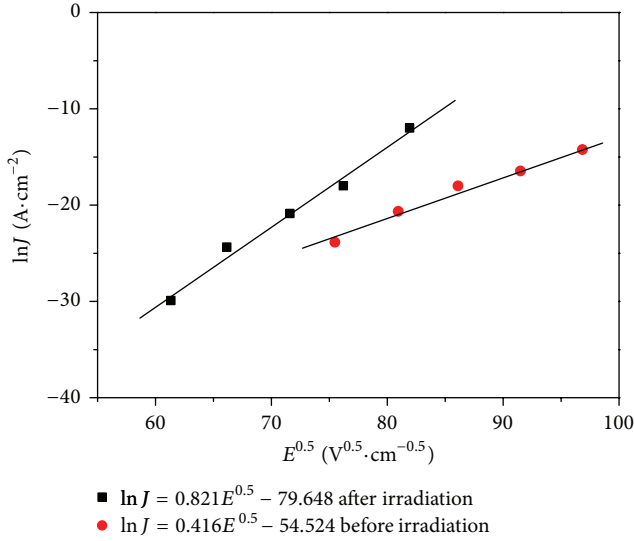
FIGURE 6: The relation patterns of $\ln J$-$E^{0.5}$ of the ZnO-based thin films before and after irradiation.

parameters were calculated by Figure 6, which were listed in Table 2, including the barrier height Φ_B, barrier width ω, interface-state density N_D, and donor concentration N_S.

Table 2 shows that after laser irradiation processing, barrier height Φ_B increased, barrier width decreased, donor concentration N_D and interface-state density N_S also increased greatly. According to [27]

$$\alpha \approx \left(\frac{\nu}{E} \right) \Phi_B^{3/2}. \quad (2)$$

Nonlinear coefficient α is proportional to potential barrier height Φ_B. Φ_B rose from 1.86 to 2.41, which prompted the increasing of α from 12.94 to 21.38. So the increasing of barrier height can effectively improve the nonlinear coefficient. According to formula $\Phi_B = e^2 N_S^2 / 2\varepsilon_0 \varepsilon_r N_D$ [18], barrier height Φ_B is closely related to the interface-state density N_S and donor concentration N_D. After laser irradiation processing, the thin film produced the lattice distortion, which increased the amount of intrinsic atomic defects of ZnO. There is no second phase diffraction peak in the X-ray diffraction patterns of samples, but which cannot exclude the doping elements as indeterminate type segregating at the grain boundaries.

4. Conclusions

After laser irradiation processing, electrical properties of the films have been improved in different degrees. The nonlinear coefficient was 24.31, which was increased by 40.8%. The breakdown voltage was 5.34 V, which was reduced by 20.7%. Leakage current density was as low as 2.03 μA/mm^2, which was reduced by 12.7%. The grain size was reduced and the clearance between the adjacent particles also decreased. The film produced the lattice distortion, prompting the increasing of ZnO intrinsic atomic defects. With the refinement of the grain, grain boundaries were increasing. In this condition, the intrinsic atomic defects of grain boundaries and Bi element segregated at the grain boundaries interact frequently, forming the composite defects of acceptor state. The interface-state density N_S of the grain boundaries increased greatly, increasing the barrier height Φ_B. Therefore, the pressure-sensitive electrical properties of ZnO-based ceramic film of laser irradiation state are excellent.
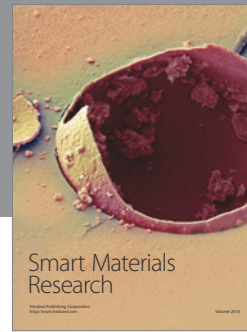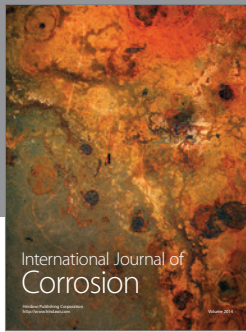
Conflict of Interests

The authors declare that there is no conflict of interests regarding the publication of this paper.

References

[1] M. Matsuoka, "Nonohmic properties of zinc oxide ceramics," *Japanese Journal of Applied Physics*, vol. 10, no. 6, pp. 736–746, 1971.

[2] T. K. Gupta, "Application of zinc oxide varistors," *Journal of the American Ceramic Society*, vol. 73, no. 7, pp. 1817–1840, 1990.

[3] D. R. Clarke, "Varistor ceramics," *Journal of the American Ceramic Society*, vol. 82, no. 3, pp. 485–502, 1999.

[4] S. Anas, R. V. Mangalaraja, M. Poothayal, S. K. Shukla, and S. Ananthakumar, "Direct synthesis of varistor-grade doped nanocrystalline ZnO and its densification through a step-sintering technique," *Acta Materialia*, vol. 55, no. 17, pp. 5792–5801, 2007.

[5] P. R. Bueno, J. A. Varela, and E. Longo, "SnO$_2$, ZnO and related polycrystalline compound semiconductors: an overview and review on the voltage-dependent resistance (non-ohmic) feature," *Journal of the European Ceramic Society*, vol. 28, no. 3, pp. 505–529, 2008.

[6] R. Puyané, "Applications and product development in varistor technology," *Journal of Materials Processing Technology*, vol. 55, no. 3-4, pp. 268–277, 1995.

[7] A. Rafferty, Y. Gun'ko, and R. Raghavendra, "An investigation of co-fired varistor-ferrite materials," *Journal of the European Ceramic Society*, vol. 24, no. 7, pp. 2005–2013, 2004.

[8] Z. N. Urgessa, O. S. Oluwafemi, and J. R. Botha, "Hydrothermal synthesis of ZnO thin films and its electrical characterization," *Materials Letters*, vol. 79, no. 15, pp. 266–269, 2012.

[9] Y. M. Li, L. H. Xu, X. G. Li, X. G. Shen, and A. L. Wang, "Effect of aging time of ZnO sol on the structural and optical properties of ZnO thin films prepared by sol-gel method," *Applied Surface Science*, vol. 256, no. 14, pp. 4543–4547, 2010.

[10] H. Z. Wu, K. M. He, D. J. Qiu, and D. M. Huang, "Low-temperature epitaxy of ZnO films on Si(001) and silica by reactive e-beam evaporation," *Journal of Crystal Growth*, vol. 217, no. 1, pp. 131–137, 2000.

[11] X. Q. Wei, J. Z. Huang, M. Y. Zhang, Y. Du, and B. Y. Man, "Effects of substrate parameters on structure and optical properties of ZnO thin films fabricated by pulsed laser deposition," *Materials Science and Engineering B*, vol. 166, no. 2, pp. 141–146, 2010.

[12] D. R. Hernández-Socorro, Z. Montiel-González, S. E. Rodil-Posada et al., "Effect of 8 MeV Si ions irradiation and thermal annealing in ZnO thin films," *Journal of Crystal Growth*, vol. 354, no. 1, pp. 169–173, 2012.

[13] N. Horio, M. Hiramatsu, M. Nawata, K. Imaeda, and T. Torii, "Preparation of zinc oxide/metal oxide multilayered thin films for low-voltage varistors," *Vacuum*, vol. 51, no. 4, pp. 719–722, 1998.

[14] W. Miśta, J. Ziaja, and A. Gubański, "Varistor performance of nanocrystalline Zn-Bi-O thin films prepared by reactive RF magnetron sputtering at room temperature," *Vacuum*, vol. 74, no. 2, pp. 293–296, 2004.

[15] M. Jiang, X. Liu, and H. Wang, "Conductive and transparent Bi-doped ZnO thin films prepared by rf magnetron sputtering," *Surface and Coatings Technology*, vol. 203, no. 24, pp. 3750–3753, 2009.

[16] Y. Zhao and Y. Jiang, "Effect of KrF excimer laser irradiation on the properties of ZnO thin films," *Journal of Applied Physics*, vol. 103, no. 11, Article ID 114903, 2008.

[17] Y. Hou and A. H. Jayatissa, "Effect of laser irradiation on gas sensing properties of sol-gel derived nanocrystalline Al-doped ZnO thin films," *Thin Solid Films*, vol. 562, no. 26, pp. 585–591, 2014.

[18] C.-Y. Tsay and M.-C. Wang, "Structural and optical studies on sol-gel derived ZnO thin films by excimer laser annealing," *Ceramics International*, vol. 39, no. 1, pp. 469–474, 2013.

[19] W. M. Tsang, F. L. Wong, M. K. Fung, J. C. Chang, C. S. Lee, and S. T. Lee, "Transparent conducting aluminum-doped zinc oxide thin film prepared by sol-gel process followed by laser irradiation treatment," *Thin Solid Films*, vol. 517, no. 2, pp. 891–895, 2008.

[20] Y. Q. Hua, G. Ji, and Z. Z. Sun, "Effect of laser shock wave on electrical property of ZnO varistor ceramics," *Laser Technology*, vol. 31, no. 1, pp. 133–136, 2011 (Chinese).

[21] I. Lorite, J. Wasik, T. Michalsky, R. Schmidt-Grund, and P. Esquinazi, "Hydrogen influence on the electrical and optical properties of ZnO thin films grown under different atmospheres," *Thin Solid Films*, vol. 556, no. 1, pp. 18–22, 2014.

[22] F. Oba and I. Tanaka, "Effect on oxidation of chemical bonding around 3d transition-metal impurities in ZnO," *Japanese Journal of Applied Physics*, vol. 38, no. 6, pp. 3570–3574, 1999.

[23] F. Oba, H. Adachi, and I. Tanaka, "Energetics and electronic structure of point defects associated with oxygen excess at a tilt boundary of ZnO," *Journal of Materials Research*, vol. 15, no. 10, pp. 2167–2175, 2000.

[24] J.-S. Jeong, "Field failure mechanism and reproduction due to moisture for low-voltage ZnO varistors," *Microelectronics Reliability*, vol. 53, no. 9–11, pp. 1632–1637, 2013.

[25] L. J. Brillson, H. L. Mosbacker, M. J. Hetzer et al., "Dominant effect of near-interface native point defects on ZnO Schottky barriers," *Applied Physics Letters*, vol. 90, no. 10, Article ID 102116, 2007.

[26] T. K. Gupta and W. G. Carlson, "A grain-boundary defect model for instability/stability of a ZnO varistor," *Journal of Materials Science*, vol. 20, no. 10, pp. 3487–3500, 1985.

[27] S. A. Pianaro, P. R. Bueno, P. Olivi, E. Longo, and J. A. Vareia, "Effect of Bi_2O_3 addition on the microstructure and electrical properties of the $SnO_2 \cdot CoO \cdot Nb_2O_5$ varistor system," *Journal of Materials Science Letters*, vol. 16, no. 8, pp. 634–638, 1997.